Carbohydrate Research 344 (2009) 627–631

Contents lists available at ScienceDirect

Carbohydrate Research

journal homepage: www.elsevier.com/locate/carres

Structural insight into the mechanism of streptozotocin inhibition of *O*-GlcNAcase

Yuan He [a], Carlos Martinez-Fleites [a], Abigail Bubb [a], Tracey M. Gloster [a,b], Gideon J. Davies [a,*]

[a] Department of Chemistry, Structural Biology Laboratory, The University of York, Heslington, York, YO10 5YW, UK
[b] Department of Chemistry, Simon Fraser University, 8888 University Drive, Burnaby, BC, V5A 1S6, Canada

ARTICLE INFO

Article history:
Received 3 November 2008
Received in revised form 2 December 2008
Accepted 3 December 2008
Available online 13 December 2008

Keywords:
Streptozotocin
O-GlcNAc
Diabetes
Inhibitor
3-D structure
Carbohydrate-active enzyme

ABSTRACT

Despite decades of its use in diabetes research, the mechanism of cytotoxicity of streptozotocin (STZ) toward pancreatic β-islet cells has remained a topic of discussion. Although STZ toxicity is likely a function of its capacity to promote DNA alkylation, it has been proposed that STZ induces pancreatic β-cell death through *O*-GlcNAcase inhibition. In this report, we explore the binding mode of STZ to a close homolog of human *O*-GlcNAcase, *Bt*GH84 from *Bacteroides thetaiotaomicron*. Our results show that STZ binds in the enzyme active site in its intact form, without the formation of a covalent adduct, consistent with solution studies on *Bt*GH84 and human *O*-GlcNAcase, as well as with structural work on a homolog from *Clostridium perfringens*. The active site of the *Bt*GH84 is considerably deformed upon STZ binding and as a result the catalytic machinery is expelled from the binding cavity.

1. Introduction

Streptozotocin (STZ; 2-deoxy-2-(3-(methyl-3-nitrosoureido)-D-glucopyranose) **1**) is a cytotoxic glucose analog that is preferentially internalized by pancreatic β-cells via the glucose transporter isoform 2 (GLUT2).[1,2] STZ has long been used to induce type I diabetes in animal models and because of its specificity to pancreatic cells, STZ is currently used in the treatment of certain pancreatic cancers (recently reviewed in Ref. 3). Despite decades of usage in diabetes research, the toxicity mechanism of STZ is not without controversy. The basis of STZ cytotoxicity has been related to its capacity to promote DNA alkylation, which in turn induces a chain of cellular processes that eventually result in cell death.[4,5] Additionally, STZ is known to be able to generate radical species such as nitrous oxide that provokes DNA damage.[6] Conversely, it has more recently been proposed that STZ exerts its toxic effects by inhibiting *O*-GlcNAcase,[7–9] the enzyme that, together with *O*-GlcNAc transferase, is responsible for the reversible intracellular *O*-GlcNAc post-translational modification.[10] The basis for this proposal is that STZ irreversibly impairs the activity of *O*-GlcNAcase leading to intracellular hyper O-GlcNAcylation of proteins, which in turn results in the onset of stress responses that ultimately may lead to apoptosis.[9] This latter proposal for the mechanism of STZ toxicity is very difficult to reconcile with reports that even more potent inhibitors of *O*-GlcNAcase are unable to replicate the cytotoxic effects of STZ despite the increased cellular *O*-GlcNAc levels they yield.[11–13] Furthermore, Macauley et al. demonstrated that STZ does not show the time-dependent inhibition of *O*-GlcNAcase that would be the signature of a covalent inactivation process.[14] In a similar vein, the van Aalten group has recently shown that when pancreatic cells are challenged with a *galacto*-configured STZ isomer, a compound that does not inhibit *O*-GlcNAcase, DNA damage and apoptosis are observed exactly as for the *gluco*-configured compound despite the lack of changes in cellular *O*-GlcNAc levels.[15]

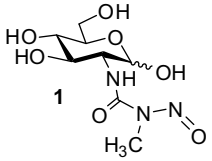

Considering the recent drive for chemical biological approaches to the study of cellular function, it is clearly imperative that the target and mode of action of small molecules are well understood. Additional efforts directed to clarify the mechanism of STZ toxicity are thus helpful to the glycobiology community. In this report, we explore the binding mode of STZ to *Bt*GH84, an *O*-GlcNAcase homolog from the human symbiont *Bacteroides thetaiotaomicron*. This enzyme serves as a good model for the human *O*-GlcNAcase, since *Bt*GH84 has active site residues that are invariant with those

* Corresponding author.
E-mail address: davies@ysbl.york.ac.uk (G.J. Davies).

0008-6215/$ - see front matter © 2008 Elsevier Ltd. All rights reserved.
doi:10.1016/j.carres.2008.12.007

expected for the human enzyme.[16] The crystal structure of the *Bt*GH84 enzyme in complex with STZ reveals an intact STZ molecule in the active site bound in a similar manner to that seen in a *Clostridium perfringens* homolog,[15] and confirms that there is neither STZ-induced covalent modification nor conversion of STZ into a potent transition state analog.[17] Intriguingly, STZ binding is also accompanied by a conformational change that flips the catalytic apparatus out of the active center reminiscent of the 'open' and 'closed' forms of the Clostridial NagJ enzyme,[18] but which had not previously been observed with *Bt*GH84.

2. Methods

2.1. X-ray crystallography

The N-terminal His_6-tagged recombinant *Bt*GH84 protein was expressed and purified as described previously.[16] Purified protein in 20 mM HEPES, pH 7.5, 300 mM NaCl was concentrated to 11 mg/mL and used for crystallization. Crystals were grown from a solution containing 15% PEG3350, 0.1 M MES, pH 6.0, 0.3 M ammonium acetate and 20% glycerol. In order to form the STZ complex, a minute amount of solid STZ was added to the crystallization mother liquor, in which crystals of *apo*-*Bt*GH84 were soaked at room temperature prior to flash freezing in liquid N_2. Diffraction data for the STZ complex were collected to 2.4 Å resolution on beamline ID23-1 of the European Synchrotron Radiation Facility (ESRF) Grenoble. Data were integrated using MOSFLM[19] and scaled and reduced with SCALA from the CCP4 suite of programs.[20] The structure of *Bt*GH84 in complex with STZ was solved using PHASER[21] with PDB entry 2CHO as the search model. Manual corrections to the model were made with COOT,[22] and refinement cycles were performed with REFMAC.[23] Water molecules and ligand were added using COOT; the stereochemical target values for the ligand were based upon ideal coordinates generated with QUANTA (Accelrys, San Diego, CA). Details of data and final structure quality are shown in Table 1. Structural figures were drawn with PYMOL[24] or BOBSCRIPT.[25] Coordinates have been deposited in the Protein Data Bank with the code 2w4x.

2.2. Isothermal titration calorimetry

Isothermal titration calorimetry (ITC) measurements were carried out using a VC calorimeter (Microcal, Northampton, MA) at 25 °C. *Bt*GH84 was dialyzed against 50 mM MES, pH 6.5, 200 mM NaCl, and concentrated to around 40 μM (measured at $A_{280\ nm}$ and calculated using a molar extinction coefficient of 140,150 $M^{-1}\,cm^{-1}$, as predicted from the protein sequence), centrifuged and degassed prior to use. STZ was diluted in the same buffer to a final concentration of 1.0 mM and degassed. Titrations were performed by injection of 10 μL aliquots of the inhibitor into the *Bt*GH84 solution. Using Microcal Origin software, the enthalpy for each injection was plotted against the molar ratio and fitted to a bimolecular model. The stoichiometry (n), enthalpy (ΔH), and association constant (K_a) were obtained from this fitting, and were used to calculate the Gibbs free energy (ΔG) and entropy ($T\Delta S$).

2.3. Enzymology

Kinetic studies of *Bt*GH84 were conducted by monitoring the change in UV–vis absorbance in thermally equilibrated disposable cuvettes using a Cintra 10 spectrophotometer. Assays were carried out at 25 °C in a total volume of 1 mL buffer (50 mM MES, pH 6.5, 200 mM NaCl) with 50 μM pNP-GlcNAc (4-nitrophenyl *N*-acetyl-D-glucosaminide) as substrate. Reactions were initiated by the addition of 10 μL of *Bt*GH84 using a syringe to a final concentration of 43 nM, and the STZ concentrations in the reaction mixture varied from 0 to 50 μM. Nitrophenolate release was recorded continuously at 400 nm for 300 s in the presence (v_i) (between 2.5 μM and 50 μM) and absence (v_o) of STZ. Reaction velocities were determined as the slope of the linear region over a 100 second period. The K_i value was calculated using the equation $v_i/v_o = 1+[I]/K_i$.

Table 1
Data collection and structure refinement statistics of the STZ complex with *Bt*GH84

Data collection	
Space group	*C*2
Cell dimensions	
a, *b*, *c* (Å)	187.0, 52.3, 84.3
α, β, γ (°)	90.0, 99.3, 90.0
Resolution (Å)	92.45–2.42 (2.55–2.42)[a]
R_{merge}	0.080 (0.511)
$I/\sigma I$	13.1 (2.6)
Completeness (%)	99.9 (99.5)
Redundancy	4.0 (3.9)
Refinement	
Resolution (Å)	2.42
No. of reflections	29526
R_{work}/R_{free}	0.18/0.24
No. of atoms	
Protein	4709
Ligand/ion	18
Water	107
B-factors (Å^2)	
Protein	26
Ligand/ion	24
Water	26
R.m.s. deviations	
Bond lengths (Å)	0.02
Bond angles (°)	1.67

[a] Values in parentheses correspond to the highest resolution shell.

3. Results and discussion

STZ is a weak (low mM) inhibitor of the human *O*-GlcNAcase.[11,14] The structural characterization of its binding mode to *O*-GlcNAcase is clearly relevant in order to distinguish between the various mechanisms through which this molecule is proposed to act. Given the practical difficulty in obtaining human *O*-GlcNAcase in a form suitable for structural work we decided to explore the structural details of STZ inhibition using a bacterial homolog to the human enzyme. *Bt*GH84 from *B. thetaiotaomicron* is known to be a valuable model to probe the structural basis of human *O*-GlcNAcase inhibition since all of its residues in the active site are predicted to be conserved in the human enzyme.[16,26] *Bt*GH84 is additionally useful in that, as is very likely in the human *O*-GlcNAcase, it possesses a cysteine residue in the active center, which is absent in the wild type NagJ GH84 enzyme (the STZ complex of which has been recently unveiled) and that might, conceivably, have been oxidized or alkylated. The inhibitory effect of STZ on the catalytic activity of *Bt*GH84 yields a low micromolar inhibition constant (10 ± 0.5 μM). Isothermal calorimetry gives a dissociation constant (K_d) of 14 ± 0.4 μM, which is consistent with the K_i value obtained by kinetic means. Binding of STZ is both enthalpically (ΔH of −4.2 ± 0.4 kcal/mol) and entropically (derived $T\Delta S$ of +2.4 kcal/mol) favorable.

The crystal structure of the STZ complex with *Bt*GH84 was solved with data to 2.42 Å resolution by molecular replacement using the coordinates of the *apo*-enzyme (PDB code 2CHO) as a search model. The enzyme crystallizes with one molecule in the *C*2 asymmetric unit, and the final model comprises protein residues Ser4-Asp589, one STZ molecule, one glycerol molecule, one calcium ion, and 107 water molecules. Residues Gly47-Lys53 are disordered and were not included in the final model. Refinement statistics are shown in Table 1. The active site of *Bt*GH84 is located in a hollow pocket at the C-terminal portion of the $(\alpha/\beta)_8$ barrel

fold.[16] Electron density in this region clearly revealed the presence of an intact STZ molecule (Fig. 1A). The pyranose ring of STZ adopts a slightly distorted $^4C_1$ chair conformation, and is bound in the active site through hydrogen bonding interactions to one water molecule and five enzyme residues, all of which are conserved between *Bt*GH84 and the human *O*-GlcNAcase. The C-1 hydroxyl group of the anomeric center is equatorial, forming a hydrogen bond with the hydroxyl group of Tyr282. Asp344 forms two hydrogen bonds with the C-4 and C-6 hydroxyl groups, and the C-3 hydroxyl group of the pyranose ring interacts with the main chain carbonyl of Gly135 and a water molecule, which in turn hydrogen bonds to the side chain of Lys166. The planar *N*-methyl-*N*-nitrosourea moiety extends into a hydrophobic pocket, where it is sandwiched between Trp337 and Tyr282. The carbonyl oxygen of this nitrosourea moiety forms a hydrogen bond with Asn339, while the STZ nitroso group interacts with Cys278.

The binding of STZ to *Bt*GH84 causes large rearrangements of various loops when compared to the structure of native *Bt*GH84 (or any other complex solved subsequently). For example, Tyr163-Ala185 shows a maximum r.m.s.d. for Cα atoms of 4.6 Å, Gly210-Leu232 of 1.6 Å and Phe240-Pro251 of 3.8 Å. All of these loops are in the vicinity of the active site, Figure 2A. Particularly, the loops that contain the catalytic machinery including residues Asp242, Asp243, and Lys166 are moved significantly with respect to other complexes, exemplified here by the recently published *Bt*GH84 complex with PUGNAc.[26] These structural rearrangements allow the accommodation of the bulky and rigid nitrosourea group and as a consequence, the active site changes its cup-like appearance to a more open and rather deformed conformation, Figure 2B and C. Interestingly, this open active site conformation observed in the *Bt*GH84 STZ complex structure resembles the *apo*-structure of the *O*-GlcNAcase NagJ homolog from *C. perfringens*.[18] That an equivalent conformational change has been observed in two independent GH84 enzymes perhaps hints at the existence of a dynamic conformational change between an 'open' form and a 'closed' form in this family of enzymes, which may have a functional significance.

In the catalytic mechanism of GH84 enzymes,[14] Asp242 (*Bt*GH84 numbering) polarises the nucleophilic acetamido group and aids the carbonyl oxygen to attack the anomeric carbon. The general acid (Asp243) facilitates cleavage of the glycosidic bond by concomitant transfer of a proton to the glycosidic oxygen. A high energy bicyclic oxazoline, or oxazolinium ion, intermediate is thus formed. In the second step of the reaction, the deprotonated aspartate (Asp243) now acts as a general base and abstracts a proton from an incoming water molecule, which attacks the anomeric center of the intermediate, causing the oxazoline ring to open. In the complexes of *Bt*GH84 with inhibitors such as PUGNAc[26] and

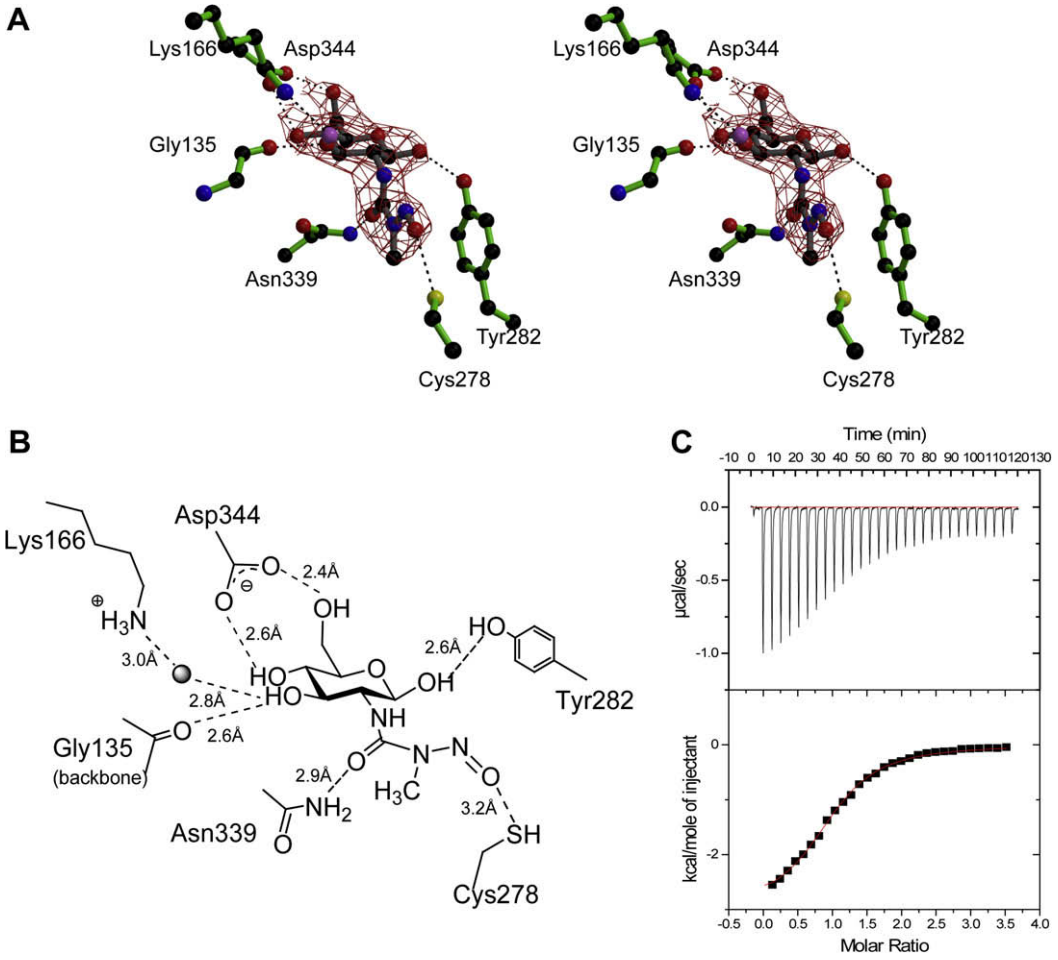

Figure 1. The 3-D structure of the STZ complex with the human *O*-GlcNAcase homolog, *Bt*GH84. (A) Stereo ball-and-stick representation of STZ bound in the active site of *Bt*GH84. The observed electron density for the maximum likelihood weighted $2F_{obs} - F_{calc}$ map is contoured at approximately 1.5σ. Spheres represent atoms of oxygen (red), nitrogen (blue), and carbon (black), and dashed lines represent hydrogen bonds. (B) Schematic representation of the interactions between STZ and *Bt*GH84; hydrogen bonds are represented by dashed lines together with their inter-atomic distances. (C) ITC data of the binding of STZ to *Bt*GH84 at 25 °C and pH 6.5. The top panel shows the raw titration data (power supplied to the system to maintain a constant temperature against time); the area of the peak gives the heat of interaction for each injection. The bottom panel shows the bimolecular fit of the normalized heats of interaction plotted against the molar concentration.

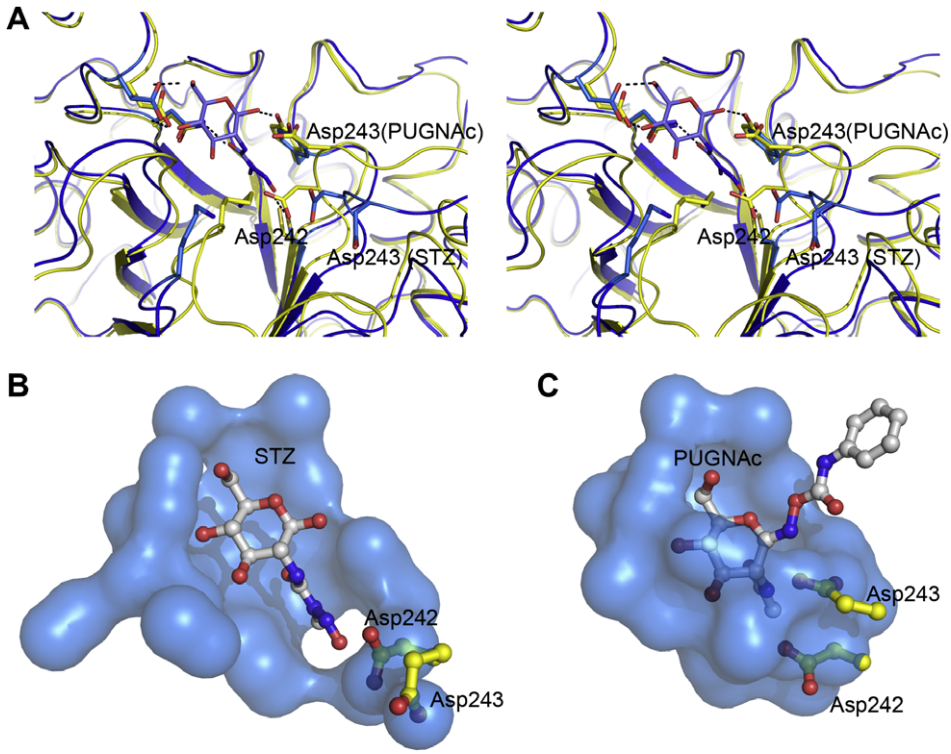

Figure 2. Conformational changes induced by STZ binding to *Bt*GH84. (A) Stereo representation of the structural superposition of the *Bt*GH84 complex with STZ (blue) and native *Bt*GH84 (yellow). Residues in direct contact with STZ are labeled. (B/C) Surface representation of the *Bt*GH84 active center with (B) STZ binding and (C) PUGNAc binding. Catalytic residues, Asp242 and Asp243, are shown in ball-and-stick representation. The pocket shape was calculated with the CASTp server.[28]

NH-butyl thiazoline,[27] the catalytic residues are within hydrogen bonding distance with their target atoms around the anomeric center as well as with the atoms in the *N*-acetyl moiety. As a result of the conformational changes in the STZ complex, however, both catalytic residues are more distant from the active center. Asp242 is some 5.3 Å away from the acetamido nitrogen and accordingly could not promote neighboring-group participation during substrate-assisted catalysis. In turn Asp243 is located about 11 Å away from the anomeric carbon. In the recently published structure of the STZ complex with the *C. perfringens* *O*-GlcNAcase homolog,[15] a similar situation is observed; the catalytic machinery is displaced from the active center but intriguingly, the overall conformation of the active site in this enzyme upon STZ binding is strikingly similar to the *apo*-structure of this enzyme (Cα r.m.s.d. 0.3 Å). In contrast, the *Bt*GH84 open conformation is observed here for the first time; the *apo*-enzyme was shown to exist in the closed conformation. These studies, therefore, reveal a hitherto unrecognized level of conformational flexibility of the active site of these enzymes.

The STZ complex structure observed here also strongly argues against two of the more obscure proposed mechanisms for how this compound inhibits *O*-GlcNAcase.[9,17] In one of these mechanisms, it is argued that STZ decomposes to form a 'transition state analog' after the loss of nitric oxide and the release of the methyl group in STZ. Here, as with the previous work on NagJ, unambiguous electron density reveals an intact and well-ordered molecule of STZ in the active site. This observation, together with the severe deformation of the active site upon STZ binding when it is compared with the active site conformation of *Bt*GH84 in complex with thiazoline-based inhibitors[16] (a compound that is geometrically similar to the putative species proposed to form on decomposition of STZ[17]), does not support any inhibitory mechanism involving formation of a transition state analog. Furthermore, past solution studies have shown that STZ does not show the time-dependent inhibition signature that such a process might imply.[14,15] Similarly, the 3-D structure argues strongly against the proposal that inhibition by STZ involves the irreversible inactivation of the human *O*-GlcNAcase through the formation of a covalent adduct, possibly via the alkylation or S-nitrosylation of the cysteine residue in the enzyme active site (Ref. 9 and references therein). In the *Bt*GH84 structure (in contrast to the recently published NagJ STZ complex where no comparable cysteine is present), residue Cys278 (which equates to Cys215 in human *O*-GlcNAcase) is found in close proximity to the nitroso group of STZ at the bottom of the active site pocket. The electron density, however, unambiguously shows that there is no covalent modification of the cysteine residue.

The use of small molecule chemical probes of cellular biology, loosely termed 'chemical biology', is clearly of increasing importance. The crux of these techniques, as with medicinal chemistry itself, is to understand the target and mode of action of any inhibitor used. Poorly understood and/or promiscuous inhibitors are likely to be highly misleading compounds which risk causing great confusion. In the case of STZ, we would argue that there is little evidence to support the continued use of this compound in studies of the *O*-GlcNAc modification. The recent evidence suggests that it is simply a poor *O*-GlcNAcase inhibitor; yet at the same time it causes cell death via a mechanism unrelated to the *O*-GlcNAc modification. Recent work has also cast some concern over the continued use of PUGNAc given its inhibitory promiscuity and potential off-target effects.[26] There is clearly considerable scope for the study of the *O*-GlcNAc modification through the use of specific chemical probes and the off-target or orthogonal effects of inhibitors should be seriously considered in future studies.

Acknowledgments

We thank the Biotechnology and Biological Sciences Research Council (BBSRC), and the University of York Wild Fund (Y.H.) for funding. G.J.D. is a Royal Society-Wolfson Research Merit Award

recipient and T.M.G. is a Wellcome Trust Sir Henry Wellcome post-doctoral fellow and a Michael Smith for Health Research trainee award holder.

References

1. Schnedl, W. J.; Ferber, S.; Johnson, J. H.; Newgard, C. B. *Diabetes* **1994**, *43*, 1326–1333.
2. Hosokawa, M.; Dolci, W.; Thorens, B. *Biochem. Biophys. Res. Commun.* **2001**, *289*, 1114–1117.
3. Lenzen, S. *Diabetologia* **2008**, *51*, 216–226.
4. Junod, A.; Lambert, A. E.; Orci, L.; Pictet, R.; Gonet, A. E.; Renold, A. E. *Proc. Soc. Exp. Biol. Med.* **1967**, *126*, 201–205.
5. Bennett, R. A.; Pegg, A. E. *Cancer Res.* **1981**, *41*, 2786–2790.
6. Kroncke, K. D.; Fehsel, K.; Sommer, A.; Rodriguez, M. L.; Kolb-Bachofen, V. *Biol. Chem. Hoppe Seyler* **1995**, *376*, 179–185.
7. Roos, M. D.; Xie, W.; Su, K.; Clark, J. A.; Yang, X.; Chin, E.; Paterson, A. J.; Kudlow, J. E. *Proc. Assoc. Am. Physicians* **1998**, *110*, 422–432.
8. Hanover, J. A.; Lai, Z.; Lee, G.; Lubas, W. A.; Sato, S. M. *Arch. Biochem. Biophys.* **1999**, *362*, 38–45.
9. Konrad, R. J.; Mikolaenko, I.; Tolar, J. F.; Liu, K.; Kudlow, J. E. *Biochem. J.* **2001**, *356*, 31–41.
10. Hart, G. W.; Housley, M. P.; Slawson, C. *Nature* **2007**, *446*, 1017–1022.
11. Gao, Y.; Parker, G. J.; Hart, G. W. *Arch. Biochem. Biophys.* **2000**, *383*, 296–302.
12. Kaneto, H.; Xu, G.; Song, K. H.; Suzuma, K.; Bonner-Weir, S.; Sharma, A.; Weir, G. C. *J. Biol. Chem.* **2001**, *276*, 31099–31104.
13. Okuyama, R.; Yachi, M. *Biochem. Biophys. Res. Commun.* **2001**, *287*, 366–371.
14. Macauley, M. S.; Whitworth, G. E.; Debowski, A. W.; Chin, D.; Vocadlo, D. J. *J. Biol. Chem.* **2005**, *280*, 25313–25322.
15. Pathak, S.; Dorfmueller, H. C.; Borodkin, V. S.; van Aalten, D. M. *Chem. Biol.* **2008**, *15*, 799–807.
16. Dennis, R. J.; Taylor, E. J.; Macauley, M. S.; Stubbs, K. A.; Turkenburg, J. P.; Hart, S. J.; Black, G. N.; Vocadlo, D. J.; Davies, G. J. *Nat. Struct. Mol. Biol.* **2006**, *13*, 365–371.
17. Toleman, C.; Paterson, A. J.; Shin, R.; Kudlow, J. E. *Biochem. Biophys. Res. Commun.* **2006**, *340*, 526–534.
18. Rao, F. V.; Dorfmueller, H. C.; Villa, F.; Allwood, M.; Eggleston, I. M.; van Aalten, D. M. *EMBO J.* **2006**, *25*, 1569–1578.
19. Leslie, A. G. W. *In Joint CCP4 and ESF-EACMB Newsletter on Protein Crystallography*, 1992, p 26.
20. Collaborative Computational Project, N. *Acta Crystallogr., Sect. D* **1994**, *50*, 760–763.
21. McCoy, A. J.; Grosse-Kunstleve, R. W.; Storoni, L. C.; Read, R. J. *Acta Crystallogr., Sect. D* **2005**, *61*, 458–464.
22. Emsley, P.; Cowtan, K. *Acta Crystallogr., Sect. D* **2004**, *60*, 2126–2132.
23. Murshudov, G. N. *Acta Crystallogr., Sect. D* **1997**, *53*, 240–255.
24. DeLano, W. L. *The PyMOL Molecular Graphics System*; DeLano Scientific: San Carlos, CA, USA, 2001.
25. Esnouf, R. M. *J. Mol. Graphics Modell.* **1997**, *15*, 132–134. 112–133.
26. Macauley, M. S.; Bubb, A.; Martinez-Fleites, C.; Davies, G. J.; Vocadlo, D. J. *J. Biol. Chem.* **2008**, *283*, 34687–34695.
27. Yuzwa, S. A.; Macauley, M. S.; Heinonen, J. E.; Shan, X.; Dennis, R. J.; He, Y.; Whitworth, G. E.; Stubbs, K. A.; McEachern, E. J.; Davies, G. J.; Vocadlo, D. J. *Nat. Chem. Biol.* **2008**, *4*, 483–490.
28. Dundas, J.; Ouyang, Z.; Tseng, J.; Binkowski, A.; Turpaz, Y.; Liang, J. *Nucleic Acids Res.* **2006**, *34*, W116–W118.